A SENSOR FOR STIFFNESS CHANGE SENSING BASED ON THREE WEAKLY COUPLED RESONATORS WITH ENHANCED SENSITIVITY

*Chun Zhao[1, *], Graham S. Wood[1], Jianbing Xie[2], Honglong Chang[2], Suan Hui Pu[1, 3], Harold M. H. Chong[1] and Michael Kraft[4]*
[1]Nano Research Group, University of Southampton, UK
[2]MOE Key Laboratory of Micro and Nano System for Aerospace, Northwestern Polytechnical University, China
[3]University of Southampton Malaysia Campus, Malaysia
[4]University of Liege, Montefiore Institute, Belgium

ABSTRACT

This paper reports on a novel MEMS resonant sensing device consisting of three weakly coupled resonators that can achieve an order of magnitude improvement in sensitivity to stiffness change, compared to current state-of-the-art resonator sensors with similar size and resonant frequency. In a 3 degree-of-freedom (DoF) system, if an external stimulus causes change in the spring stiffness of one resonator, mode localization occurs, leading to a drastic change of mode shape, which can be detected by measuring the modal amplitude ratio change. A 49 times improvement in sensitivity compared to a previously reported 2DoF resonator sensor, and 4 orders of magnitude enhancement compared to a 1DoF resonator sensor has been achieved.

INTRODUCTION

Over the last couple of decades, micro- and nano-fabricated resonant devices have been widely used to sense small changes in the properties of the resonator [1]. Among these, sensing devices that detect stiffness change have been used for many applications, such as accelerometers [2], imaging microscopy [3] and others.

For sensing a change in stiffness, an amplitude modulation sensing paradigm with two weakly coupled resonators [4] was previously proposed to enhance the sensitivity compared to conventional single resonator sensors with frequency shift as output [5]. By combining two identical resonators and a weak coupling element in between, the change in mode shapes is more pronounced than the shift in frequency for the same stiffness perturbation [6].

The device reported here employed a novel approach based on three weakly coupled resonators arranged in a chain. Unlike previous work using 2DoF resonators, for which identical resonators were used, we intentionally designed the suspension system of the middle resonator stiffer than that of the other two identical resonators; in this way, an enhancement in sensitivity could be achieved [7].

THEORY

System Model

The lumped parameter block diagram of a 3DoF resonator system is shown in Fig. 1. Each resonator is modelled as a mass and spring; damping is neglected for the analysis. The springs between the resonators are the coupling springs.

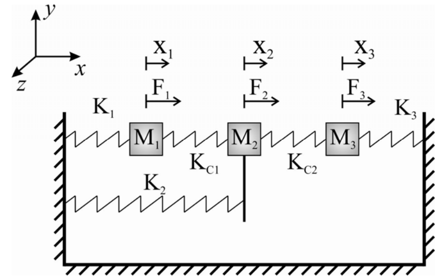

Figure 1: Mass-damper-spring lumped parameter model of a 3DoF resonator sensing device

Suppose the mass of all resonators are identical, i.e. $M_1=M_2=M_3=M$, the two coupling springs are also identical, $K_{c1}=K_{c2}=K_c$, whereas the spring stiffness of the resonators are asymmetrical with $K_1=K$, $K_3=K+\Delta K$. In addition, the stiffness of the resonator in the middle is K_2. Further, assuming all springs are linear, and no movement in the y and z-axis, the equations of motions in the x-axis after Laplace transform are given by:

$$H_1(s)X_1(s) = F_1(s) + K_c X_2(s) \tag{1}$$

$$H_2(s)X_2(s) = F_2(s) + K_c[X_1(s) + X_3(s)] \tag{2}$$

$$H_3(s)X_3(s) = F_3(s) + K_c X_2(s) \tag{3}$$

where the transfer functions are defined as:

$$H_1(s) = Ms^2 + K + K_c \tag{4}$$

$$H_2(s) = Ms^2 + K_2 + 2K_c \tag{5}$$

$$H_3(s) = Ms^2 + K + K_c + \Delta K \tag{6}$$

If the system is actuated by $F_1(s)$ only, the displacement $X_1(s)$ and $X_3(s)$ can be computed as a function of $F_1(s)$:

$$X_1(s) = \frac{F_1(s)[H_2(s)H_3(s) - K_c^2]}{H_1(s)H_2(s)H_3(s) - K_c^2[H_1(s) + H_3(s)]} \tag{7}$$

$$X_3(s) = \frac{F_1(s)K_c^2}{H_1(s)H_2(s)H_3(s) - K_c^2[H_1(s) + H_3(s)]} \tag{8}$$

In the ideal case with negligible damping and $\Delta K=0$, there are three distinctive modes: in the first mode, all three resonators vibrate in-phase; in the second mode, resonators 1 and 3 are out-of-phase, with the resonator in the middle being stationary; in the third mode, resonators 1 and 3 are in-phase, but are out-of-phase with respect to resonator 2 [8]. When a perturbation in stiffness is introduced, $\Delta K \neq 0$, the three modes are disturbed resulting in amplitude changes and mode localization occurs [9]. The modes of interest in this work are the first two modes due to higher sensitivity than the third mode, which will be referred to as in-phase and out-of-phase modes, respectively.

In this work, the amplitude ratio $|X_1(s)/X_3(s)|$ is used to gauge the mode localization caused by stiffness perturbation.

Amplitude Ratio and Sensitivity Analysis

Assuming a weak coupling stiffness of $K_c<K/10$ and the stiffness of resonator 2 being more than twice than that of resonator 1, so that the following condition is satisfied:

$$|K_c| < \frac{K}{10} < \frac{K_2 - K}{10} \tag{9}$$

Let $s=j\omega$, the frequencies of the in-phase and out-of-phase modes can be approximated as:

$$\omega_{ip} \approx \sqrt{\frac{1}{M}[K + K_c + \frac{1}{2}(\Delta K - \alpha - \sqrt{\Delta K^2 + \alpha^2})]} \tag{10}$$

$$\omega_{op} \approx \sqrt{\frac{1}{M}[K + K_c + \frac{1}{2}(\Delta K - \alpha + \sqrt{\Delta K^2 + \alpha^2})]} \tag{11}$$

where ω_{ip} and ω_{op} denote the frequencies of the in-phase and out-of-phase modes, respectively, and

$$\alpha = \frac{2K_c^2}{K_2 - K + K_c} \tag{12}$$

Substituting (10) and (11) into (7) and (8), we can estimate the amplitude ratios for the in-phase and out-of-phase modes as:

$$\left|\frac{X_1(j\omega_{ip})}{X_3(j\omega_{ip})}\right| \approx \left|\frac{\sqrt{\gamma_3^2(\Delta K/K)^2 + 4} + \gamma_3(\Delta K/K)}{2}\right| \tag{13}$$

$$\left|\frac{X_1(j\omega_{op})}{X_3(j\omega_{op})}\right| \approx \left|-\frac{\sqrt{\gamma_3^2(\Delta K/K)^2 + 4} - \gamma_3(\Delta K/K)}{2}\right| \tag{14}$$

where,

$$\gamma_3 = \frac{2K}{\alpha} = \frac{K(K_2 - K + K_c)}{K_c^2} \tag{15}$$

To verify the results, an equivalent electrical RLC model was constructed as shown in Figure 2 [8].

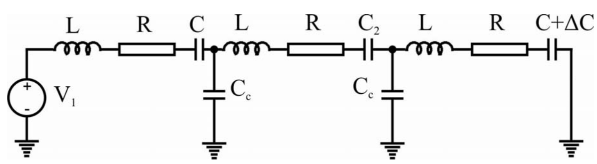

Figure 2: Equivalent RLC model of a 3DoF resonator system

The electrical model was simulated using values listed in Table 1 representing our designed device. Small resistors were added so that the PSpice simulation converges. The resulting simulated quality factor was 10^5, which is a good approximation of the undamped system. The simulated resonant frequencies are compared to theoretical values calculated using (10) and (11) in Figure 3, and the theoretical amplitude ratios computed by (13) and (14) are verified in Figure 4.

Table 1: Values used in the simulation of the electrical equivalent model

Component	Value	Mechanical model equivalent
L	0.489MH	M
C	0.254fF	K
C_2	84.8aF	$K_2/K=3$
C_c	19.07fF	K/K_c75, γ_3=11324
R	0.44MΩ	$Q=10^5$
ω_0	14.27kHz	Resonant frequency of single resonator

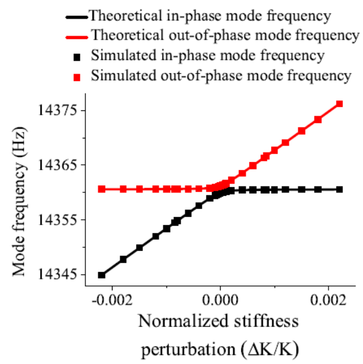

Figure 3: Simulation results showing the in-phase (black) and out-of-phase (red) mode frequencies as a function of a normalized stiffness perturbation. The theoretically calculated mode frequencies match well with the simulated values.

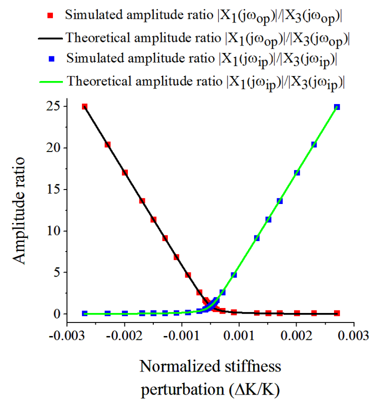

Figure 4: Simulated and calculated (using (13) and (14)) amplitude ratios of in-phase and out-of-phase modes as a function of normalized stiffness perturbation. The theoretically calculated amplitude ratios match well with simulated values.

It can be seen from Figures 3 and 4 that the theoretical estimations of mode frequencies and amplitude ratios match well with the simulated results (within 1%).

Due to the symmetry as shown in Figure 4, without loss of generality, the amplitude ratio of the out-of-phase mode for $\Delta K/K<0$ is chosen for the following sensitivity analysis.

It can be seen from Figure 4 that for negative stiffness perturbations the amplitude ratio is approximately a linear function of stiffness perturbation. Assuming $|\gamma_3\Delta K/K|>10$, the mathematical amplitude ratio

(14) can be linearized as:

$$\left|\frac{X_1(j\omega_{op})}{X_3(j\omega_{op})}\right| \approx -\frac{\gamma_3 \Delta K}{K} \tag{16}$$

The linear sensitivity of the sensor (the ratio of the change in amplitude ratio to the normalized stiffness change) can therefore be expressed as:

$$S_{3DoF} = \partial\left(\left|\frac{X_1(j\omega_{op})}{X_3(j\omega_{op})}\right|\right) \Big/ \partial\left(\frac{\Delta K}{K}\right) \approx -\gamma_3 \tag{17}$$

where γ_3 is defined in (15).

EXPERIMENTAL RESULTS

Device Fabrication

A 3DoF resonator device was fabricated using a single mask silicon-on-insulator (SOI) process with a structural layer of 30µm thickness. The process involves the following steps: 1) photoresist deposition and patterning; 2) DRIE etching of the device layer to define the structure; 3) overetch by DRIE, utilizing the notching effect to dry-release the majority of the proof mass, thereby avoiding stiction of the proof mass to the handle wafer during the wet release step; 4) removing the photoresist, followed by dicing; 5) HF wet release the resonator structures. A summary of the process flow is shown in Figure 5, a more detailed description is provided in [10].

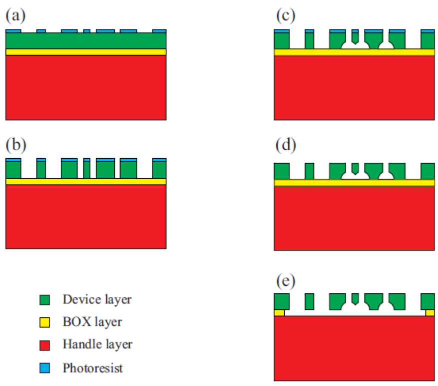

Figure 5: The process flow of the single mask SOI process: a) deposition and patterning of photoresist, b) DRIE etching, c) overetching, d) photoresist removal and dicing, e) HF solution release.

An SEM micrograph of a fabricated chip of the 3DoF MEMS resonator sensor is shown in Figure 6.

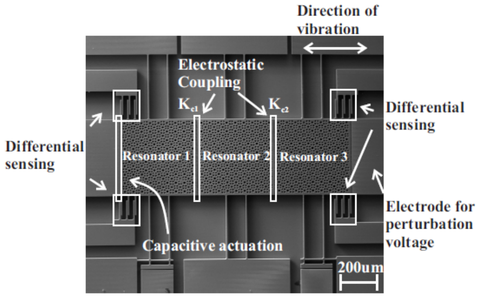

Figure 6: SEM image of a micro-fabricated prototype 3DoF resonator sensing device

Experimental Configuration

The system consists of three resonators. Electrostatic springs were used as coupling elements between the resonators [6], allowing variable coupling strength. Identical bias voltages of 30V were applied to resonators 1 and 3, whereas resonator 2 was grounded, to ensure $K_{c1}=K_{c2}$. To demonstrate the sensitivity of the 3DoF device to stiffness perturbations, another variable DC voltage was applied on the electrode on the right. Actuation of the resonators was realized by applying an AC voltage to the electrode on the left. Differential motional currents were obtained through the differential sensing comb fingers attached to resonators 1 and 3. The configuration of the device for characterization is shown in Figure 7.

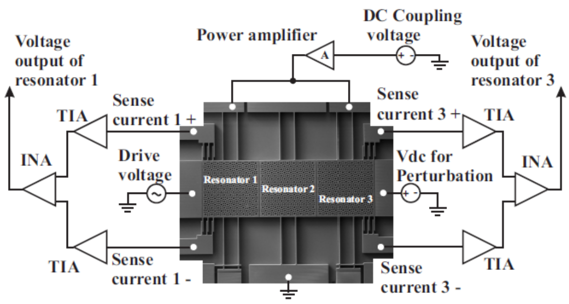

Figure 7: Test configuration of the prototype 3DoF resonator sensing device

The chip was wire bonded to the contacts of a chip carrier, and tested electrically on printed circuit board, which consisted of standard transimpedance amplifiers (TIA) and instrumentation amplifiers (INA). The chip and the circuit board were placed into a customized vacuum chamber with electrical feedthroughs. The ambient pressure for the testing was 20µTorr, so a high quality factor could be obtained. The experimental set-up is shown in Figure 8.

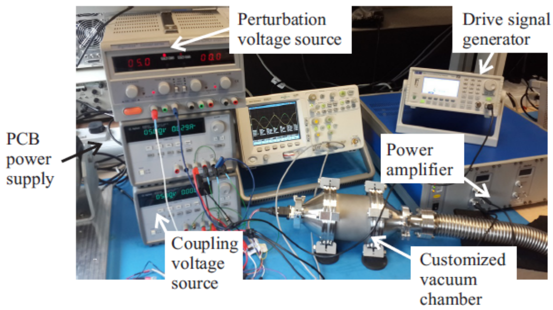

Figure 8: Experimental set up for 3DoF sensor characterization

RESULTS AND DISCUSSION

Frequency Response

The frequency response of the device was measured with various perturbation voltages applied. A typical frequency response of resonators 1 and 3 of the sensing device is shown in Figure 9. The measured 3-dB bandwidth and the quality factor of the out-of-phase mode were 2.40Hz and 6221, respectively. The frequency difference between the in-phase and out-of-phase modes was 4.99Hz, which is greater than twice of the 3-dB bandwidth of the out-of-phase mode, indicating weak damping, which thus can be neglected.

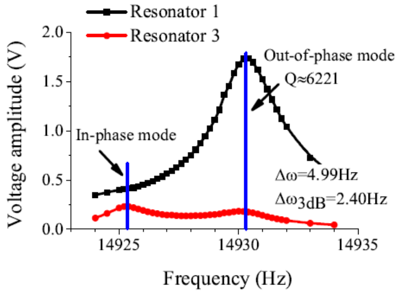

Figure 9: Typical frequency response of resonators 1 and 3, with 30V coupling voltage and 4.15V perturbation voltage.

Sensitivity

Upon finding the mode frequency of the out-of-phase mode, mode amplitudes of resonators 1 and 3 were averaged and recorded. The amplitude ratios of the out-of-phase mode were then computed. Figure 10 shows the measured amplitude ratio (quotient of modal amplitudes of resonators 1 and 3) at the out-of-phase mode for different stiffness perturbations with 30V coupling voltage. The measurement results are presented together with a linear fit. The linear sensitivity to normalized stiffness change extracted from the measured data was found to be 13558, whereas the theoretical calculated value was 17073. The discrepancy was due to fabrication variances. Table 1 lists a comparison of sensitivity between state-of-the-art resonator sensors (1Dof and 2DoF) for stiffness change sensing and our work.

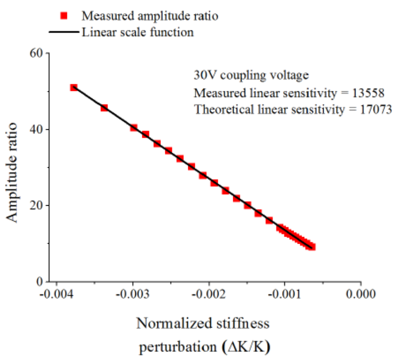

Figure 10: Measured amplitude ratio at the out-of-phase mode of the 3DoF resonator sensor, for different stiffness perturbations.

Table 2: Sensitivity comparison

Reference	Sensor output	Measured sensitivity	Sensor type
[5]	Frequency shift	0.5	Single resonator
[6]	Eigenstate shift	275	Two resonators
This work	Amplitude ratio change	13558	Three resonators

CONCLUSIONS AND OUTLOOK

In this paper, we have reported a novel 3DoF resonator device for stiffness change sensing applications. The measured sensitivity of a prototype sensor represents an improvement by over 49 times compared to the state-of-the-art stiffness change sensors consisting of two weakly coupled resonators. In the future, the effect of damping will be included in the analysis. In addition, other specifications of the sensor, such as dynamic range, linearity and resolution will also be investigated.

ACKNOWLEDGEMENT

The authors would like to thank the support from the Programme of Introducing Talents of Discipline to Universities, China (Grant No.B13044).

REFERENCES

[1] M. Schmidt and R.T. Rowe, “Silicon resonant microsensors,” *14th Automotive Materials Conference: Ceramic Engineering and Science Proceedings*, Volume 8, Issue 9/10, pages 1019–1034. Wiley Online Library.

[2] A. Seshia, M. Palaniapan, T.A Roessig, R.T. Howe, R. W. Gooch, T. R. Schimert, and S. Montague, “A vacuum packaged surface micromachined resonant accelerometer,” *Microelectromechanical Systems, Journal of*, 11(6):784–793, Dec 2002.

[3] U. Durig, J. K. Gimzewski and D. W. Pohl, “Experimental Observation of Forces Acting during Scanning Tunneling Microscopy”, *Phys. Rev. Lett.*, 57:2403–2406, Nov 1986.

[4] M. Spletzer, A. Raman, A. Q. Wu, X. Xu and R. Reifenberger, “Ultrasensitive mass sensing using mode localization in coupled microcantilevers”, *Applied Physics Letters*, 88, 254102, 2006.

[5] F. J. Giessibl, “A direct method to calculate tip–sample forces from frequency shifts in frequency-modulation atomic force microscopy”, *Applied Physics Letters*, 78(1), 2001.

[6] P. Thiruvenkatanathan, J. Yan and A. A. Seshia, “Ultrasensitive mode-localized micromechanical electrometer,” In *Frequency Control Symposium (FCS), 2010 IEEE International*, pages 91–96, June 2010.

[7] C. Zhao, G. S. Wood, S. H. Pu and M. Kraft, “Design of an ultra-sensitive MEMS force sensor utilizing mode localization in weakly coupled resonators”, In *23rd MME Workshop, 2012.*

[8] C. T.-C. Nguyen, “Frequency-selective mems for miniaturized low-power communication devices,” *Microwave Theory and Techniques, IEEE Transactions on, 47(8):1486–1503, Aug 1999.*

[9] C. Pierre, “Mode localization and eigenvalue loci veering phenomena in disordered structures,” *Journal of Sound and Vibration, 126(3):485 – 502, 1988.*

[10] J. B. Xie, Y. C. Hao, H. L. Chang, and W. Z. Yuan, “Single mask selective release process for complex soi mems device,” *Key Engineering Materials, 562:1116–1121, 2013.*

CONTACT

*Chun Zhao, tel: +44 77 30043696; cz1y10@soton.ac.uk